

Hybrid Beamforming Optimization for DOA Estimation Based on the CRB Analysis

Tian Lin, Xuemeng Zhou, Yu Zhu, and Yi Jiang

Abstract—Direction-of-arrival (DOA) estimation is one of the most demanding tasks for the millimeter wave (mmWave) communication of massive multiple-input multiple-output (MIMO) systems with the hybrid beamforming (HBF) architecture. In this paper, we focus on the optimization of the HBF matrix for receiving pilots to enhance the DOA estimation performance. Motivated by the fact that many existing DOA estimation algorithms can achieve the Cramér-Rao bound (CRB), we formulate the HBF optimization problem aiming at minimizing the CRB with the prior knowledge of the rough DOA range. Then, to tackle the problem with intractable non-convex constraint introduced by the analog beamformers, we propose an efficient manifold optimization (MO) based algorithm. Simulation results demonstrate the significant improvement of the proposed CRB-MO algorithm over the conventional random HBF algorithm, and provide insights for the HBF design in the beam training stage for practical applications.

Index Terms—Hybrid beamforming, Cramér-Rao bound, direction-of-arrival estimation, manifold optimization.

I. INTRODUCTION

Hybrid beamforming (HBF) is regarded as a promising technology for millimeter wave (mmWave) massive multiple-input multiple-output (MIMO) communication systems due to its advantage of achieving considerable beamforming gains with much lower hardware cost and power consumption when compared with the fully digital beamforming [1], [2]. However, its performance heavily relies on the accuracy of direction-of-arrival (DOA) estimation. There have been many works focusing on the design of DOA estimation algorithms with the HBF architecture. For example, an algorithm using the two-dimension (2D) discrete Fourier transform (DFT) approach has been proposed in [3]. Subsequently, a fast root multiple signal classification (root-MUSIC) algorithm has been developed in [4] by extending the conventional MUSIC algorithm.

For massive MIMO systems, the hybrid beamformers of high dimensions are endowed with sufficient freedom to customize the baseband pilots and benefit the subsequent DOA estimation. However, most related works simply adopted the random hybrid beamformers or DFT based hybrid beamformers for DOA measurements [3]–[6], which requires a large number of training pilots to guarantee good performance. In this letter we investigate the DOA estimation and optimize the HBF to improve the performance based on the Cramér-Rao bound (CRB) analysis with the utilization of the prior

information of the DOA range. Our contributions can be summarized as follows:

- Recognizing that many existing estimation algorithms, e.g., [4], [7], perform closely to the CRB, we propose to optimize HBF aiming at minimizing the CRB. The simulation results verify that our optimized HBF can improve the performance of existing DOA estimation algorithms.
- As there is usually some prior information about the (rough) range of DOA, we elaborate how to utilize the prior information to specify the optimization objective for better performance.
- Due to the partially-connected (PC) HBF architecture and the implementation of the phase shifters, the feasible region of the CRB minimization problem is non-convex, which complicates the solution. To tackle the highly non-convexity, we propose an efficient manifold optimization (MO) based algorithm with guaranteed convergence.

Notations: Matrices and vectors are denoted by boldface capital and lower-case letters, respectively. $[\mathbf{a}]_i$ denotes the i -th entry of a vector. $[\mathbf{A}]_{ij}$ denotes the (i, j) -th entry of a matrix. $(\cdot)^*$, $(\cdot)^T$, and $(\cdot)^H$ denote the complex conjugate, transpose, complex conjugate transpose of a matrix or vector. $d(\mathbf{A})$ denotes the differential of \mathbf{A} . $\text{tr}(\cdot)$, $\|\cdot\|_F$, and $\text{Re}(\cdot)$ denote the trace, the Frobenius norm, and of the real part of a matrix, respectively. $\text{diag}(\mathbf{x})$ is a diagonal matrix with the entries of \mathbf{x} on its main diagonal and $\text{blkdiag}(\mathbf{X}_1, \dots, \mathbf{X}_n)$ denotes a block diagonal matrix whose diagonal components are $\mathbf{X}_1, \dots, \mathbf{X}_n$. $\mathcal{CN}(\mathbf{0}, \mathbf{K})$ denotes the circularly symmetric complex Gaussian distribution with zero mean and covariance matrix \mathbf{K} . \otimes and \odot denote the Kronecker product and the Hadamard product, respectively.

II. SYSTEM MODEL

Consider the DOA estimation in the uplink of a block-fading mmWave MIMO communication system, where a base station (BS) is equipped with a large number (N_{BS}) of antennas and adopts the PC-HBF architecture to reduce the hardware cost, and a user equipment (UE) is equipped with a small number (N_{UE}) of antennas and adopts the fully digital beamforming. Define the transmitted training sequence at the UE as $\mathbf{s} = [s_0, \dots, s_{N-1}]^T$, where N is the length and $|s_n| = 1$. As the training sequence \mathbf{s} are being beamformed by $\mathbf{v} \in \mathbb{C}^{N_{\text{UE}}}$, the equivalent baseband received signal at the BS antenna array is given by [8], [9]

$$\mathbf{r}_n = \mathbf{H}\mathbf{v}s_n + \mathbf{z}_n, \quad \text{for } n = 0, \dots, N-1, \quad (1)$$

This work was supported by National Natural Science Foundation of China under Grant No. 61771147 and No. 61771005.

The authors are with the Key Laboratory for Information Science of Electromagnetic Waves (MoE), School of Information Science and Technology, Fudan University, Shanghai 200433, China. (e-mail: lint17@fudan.edu.cn, xuemeng19@fudan.edu.cn, zhuyu@fudan.edu.cn, jiangyi@fudan.edu.cn).

where \mathbf{z}_n denotes the additive Gaussian noise vector with $\mathbf{z}_n \sim \mathcal{CN}(\mathbf{0}, \sigma^2 \mathbf{I}_{N_{\text{BS}}})$ and σ^2 represents the noise variance, the transmit power is represented by $P = \|\mathbf{v}\|^2$. \mathbf{H} is the mmWave MIMO channel matrix and assumed unchanged during the whole training process. Normally \mathbf{H} can be characterized by the geometry-based channel model as follows

$$\mathbf{H} = \sqrt{\frac{N_{\text{BS}} N_{\text{UE}}}{L}} \sum_{l=0}^{L-1} \alpha_l \mathbf{a}_{\text{BS},l}(\theta_l, \phi_l) \mathbf{a}_{\text{UE},l}^H(\psi_l, \gamma_l), \quad (2)$$

where L is the number of propagation paths and $l=0$ denotes the line-of-sight (LoS) link which has the strongest gain. Furthermore, α_l is the complex path gain of the l -th path, $\mathbf{a}_{\text{BS},l}$ and $\mathbf{a}_{\text{UE},l}$ represent the antenna array response vectors of the BS and the UE, respectively. $\theta_l(\phi_l)$ denotes the associated azimuth (elevation) angle of arrival, and $\psi_l(\gamma_l)$ denotes the associated azimuth (elevation) angle of departure, respectively. Given that a uniform planar array (UPA) of $P \times Q$ elements is deployed at the BS, the array response is [1], [2]

$$\mathbf{a}_{\text{BS},l}(\theta_l, \phi_l) = \mathbf{a}_y(\theta_l, \phi_l) \otimes \mathbf{a}_z(\phi_l), \quad (3)$$

where $\mathbf{a}_y(\theta_l, \phi_l) = \frac{1}{\sqrt{Q}} [1, e^{j\pi \sin \theta_l \sin \phi_l}, \dots, e^{j\pi(Q-1) \sin \theta_l \sin \phi_l}]^T$ and $\mathbf{a}_z(\phi_l) = \frac{1}{\sqrt{P}} [1, e^{j\pi \cos \phi_l}, \dots, e^{j\pi(P-1) \cos \phi_l}]^T$. Denote the hybrid combiner at the BS as $\mathbf{W}_n = \mathbf{W}_{\text{RF},n} \mathbf{W}_{\text{BB},n} \in \mathbb{C}^{N_{\text{BS}} \times N_{\text{RF}}}$, where $\mathbf{W}_{\text{RF},n} \in \mathbb{C}^{N_{\text{BS}} \times N_{\text{RF}}}$ denotes the analog combiner and $\mathbf{W}_{\text{BB},n} \in \mathbb{C}^{N_{\text{RF}} \times N_{\text{RF}}}$ denotes the digital baseband one. Then, the combined signal at time instance n can be represented as

$$\mathbf{y}_n = \mathbf{W}_n^H \mathbf{r}_n = \mathbf{W}_n^H \mathbf{H} \mathbf{v}_s + \mathbf{W}_n^H \mathbf{z}_n. \quad (4)$$

It should be mentioned that due to the implementation of phase shifters in the PC-HBF architecture, $\mathbf{W}_{\text{RF},n} = \text{blkdiag}(\mathbf{w}_{n,1}, \dots, \mathbf{w}_{n,N_{\text{RF}}})$, where $\mathbf{w}_{n,m}$, for $m = 1, \dots, N_{\text{RF}}$, is an $\frac{N_{\text{BS}}}{N_{\text{RF}}} \times 1$ column vector with its elements having a unit modulus, i.e., $|\mathbf{w}_{n,m}|_i = 1, \forall n, m, i$ [1], [4].

III. CRB ANALYSIS AND PROBLEM FORMULATION

Inspired by the fact that the existing DOA estimation algorithm can closely approach the CRB [4], [6], [7], we propose to optimize the hybrid combiner with the objective of minimizing the CRB. In this section we first analyze the CRB with HBF, and then formulate the HBF optimization problem for DOA estimation.

To simplify the analysis, we recognize that the downlink mmWave transmission is usually dominated by the LoS path due to its much higher gain compared with the none LoS (NLoS) paths [10]. Thus, in the following derivation, we focus on the estimation of the DOA of the LoS path and ignore the effect of the NLoS paths. However, such effect will be considered in the simulation.

A. CRB Analysis

As the training sequence is known at both the BS and the UE, we have

$$\tilde{\mathbf{y}}_n = \mathbf{y}_n s_n^* = \beta \mathbf{W}_n^H \mathbf{a}_{\text{BS}}(\theta, \phi) + \mathbf{W}_n^H \tilde{\mathbf{z}}_n, \quad (5)$$

where the subscript $(\cdot)_0$ of the channel parameters of the LoS path is omitted for simplicity, $\beta = \alpha \mathbf{a}_{\text{UE}}^H(\psi, \gamma) \mathbf{v}$, and $\tilde{\mathbf{z}}_n =$

$s_n^* \mathbf{z}_n$ has the same distribution as \mathbf{z}_n . By collecting $\tilde{\mathbf{y}}_n$ for $n = 0, \dots, N-1$, we have

$$\tilde{\mathbf{y}} = \beta \mathbf{W}^H \mathbf{a}_{\text{BS}}(\theta, \phi) + \widehat{\mathbf{W}}^H \tilde{\mathbf{z}}, \quad (6)$$

where $\tilde{\mathbf{y}} = [\tilde{\mathbf{y}}_0^T, \dots, \tilde{\mathbf{y}}_{N-1}^T]^T$, $\mathbf{W} = [\mathbf{W}_0, \dots, \mathbf{W}_{N-1}]$, $\widehat{\mathbf{W}} = \text{blkdiag}(\mathbf{W}_0, \dots, \mathbf{W}_{N-1})$, and $\tilde{\mathbf{z}} = [\tilde{\mathbf{z}}_0^T, \dots, \tilde{\mathbf{z}}_{N-1}^T]^T$. To derive the CRB, first define $\boldsymbol{\eta} \triangleq [\theta, \phi, \text{Re}\{\beta\}, \text{Im}\{\beta\}]$ as the vector containing the parameters to be estimated. As $\tilde{\mathbf{y}} \sim \mathcal{CN}(\beta \mathbf{W}^H \mathbf{a}_{\text{BS}}(\theta, \phi), \sigma^2 \widehat{\mathbf{W}}^H \widehat{\mathbf{W}})$, according to [11], the Fisher information matrix (FIR) can be derived as follows

$$\mathbf{F} = \frac{2}{\sigma^2} \text{Re}\{\mathbf{A}^H \mathbf{W} (\widehat{\mathbf{W}}^H \widehat{\mathbf{W}})^{-1} \mathbf{W}^H \mathbf{A}\}, \quad (7)$$

where $\mathbf{A} = \frac{\partial(\beta \mathbf{a}_{\text{BS}}(\theta, \phi))}{\partial \boldsymbol{\eta}}$ is an $N_{\text{BS}} \times 4$ matrix and is given by

$$\mathbf{A} = [\beta \mathbf{a}_1, \beta \mathbf{a}_2, \mathbf{a}_{\text{BS}}(\theta, \phi), \mathbf{j} \mathbf{a}_{\text{BS}}(\theta, \phi)], \quad (8)$$

where

$$\begin{aligned} \mathbf{a}_1 &= \left(j\pi \cos \theta \sin \phi [0, 1, \dots, Q-1]^T \odot \mathbf{a}_y(\theta, \phi) \right) \otimes \mathbf{a}_z(\phi) \\ \mathbf{a}_2 &= \left(j\pi \sin \theta \cos \phi [0, 1, \dots, Q-1]^T \odot \mathbf{a}_y(\theta, \phi) \right) \otimes \mathbf{a}_z(\phi) \\ &\quad + \mathbf{a}_y(\theta, \phi) \otimes \left(-j\pi \sin \phi [0, 1, \dots, P-1]^T \odot \mathbf{a}_z(\phi) \right). \end{aligned}$$

Recalling that $\mathbf{W}_n = \mathbf{W}_{\text{RF},n} \mathbf{W}_{\text{BB},n}$, we have

$$\mathbf{W} = \mathbf{W}_{\text{RF}} \mathbf{W}_{\text{BB}}, \quad \widehat{\mathbf{W}} = \widehat{\mathbf{W}}_{\text{RF}} \mathbf{W}_{\text{BB}}, \quad (9)$$

where $\mathbf{W}_{\text{RF}} = [\mathbf{W}_{\text{RF},0}, \dots, \mathbf{W}_{\text{RF},N-1}] \in \mathbb{C}^{N_{\text{BS}} \times N_{\text{RF}} N}$, $\mathbf{W}_{\text{BB}} = \text{blkdiag}(\mathbf{W}_{\text{BB},0}, \dots, \mathbf{W}_{\text{BB},N-1}) \in \mathbb{C}^{N_{\text{RF}} N \times N_{\text{RF}} N}$, and $\widehat{\mathbf{W}}_{\text{RF}} = \text{blkdiag}(\mathbf{W}_{\text{RF},0}, \dots, \mathbf{W}_{\text{RF},N-1}) \in \mathbb{C}^{N_{\text{BS}} N \times N_{\text{RF}} N}$. By substituting (9) into (7), we find that \mathbf{F} can be simplified as

$$\mathbf{F} = \frac{2N_{\text{RF}}}{\sigma^2 N_{\text{BS}}} \text{Re}\{\mathbf{A}^H \mathbf{W}_{\text{RF}} \mathbf{W}_{\text{RF}}^H \mathbf{A}\}, \quad (10)$$

which follows from the fact that \mathbf{W}_{BB} is an invertible matrix and $\widehat{\mathbf{W}}_{\text{RF}}^H \widehat{\mathbf{W}}_{\text{RF}} = \frac{N_{\text{BS}}}{N_{\text{RF}}} \mathbf{I}$. Then, the CRB matrix $\mathbf{C} = \mathbf{F}^{-1}$, where the diagonal elements reveal the minimum variances of the associated estimates. As we focus on the estimation of θ and ϕ , we are interested in the left-top 2×2 sub-matrix of \mathbf{C} , which is denoted by \mathbf{C}_{11} . By rewriting \mathbf{F} as a block matrix, we have

$$\mathbf{F} = \begin{bmatrix} \mathbf{F}_{11} & \mathbf{F}_{12} \\ \mathbf{F}_{21} & \mathbf{F}_{22} \end{bmatrix}, \quad \mathbf{C}_{11} = (\mathbf{F}_{11} - \mathbf{F}_{12} \mathbf{F}_{22}^{-1} \mathbf{F}_{21})^{-1}, \quad (11)$$

where $\mathbf{F}_{mn} = \text{Re}\{\mathbf{A}_m^H \mathbf{W}_{\text{RF}} \mathbf{W}_{\text{RF}}^H \mathbf{A}_n\}$ for $m, n = \{1, 2\}$, and \mathbf{A}_1 and \mathbf{A}_2 are defined as the sub-matrices containing the first two columns and the last two columns of \mathbf{A} in (8), respectively.

B. Problem Formulation

From (11), we see that the CRB is a function of \mathbf{W}_{RF} . Thus, one can improve the estimation performance via optimizing \mathbf{W}_{RF} to minimize the CRB. That is, to solve

$$\mathbf{W}_{\text{RF},\text{opt}} = \arg \min_{\mathbf{W}_{\text{RF}}} \text{tr}(\mathbf{C}_{11}). \quad (12)$$

The CRB, however, is associated with the unknown β and DOA, and thus cannot be directly used as the objective function. Nevertheless, we first propose the following lemma:

Lemma 1 *The solution of (12) is independent of β .*

Proof: According to (7) and the definition of \mathbf{F}_{mn} , both \mathbf{F}_{11} and $\mathbf{F}_{12}\mathbf{F}_{22}^{-1}\mathbf{F}_{21}$ in (11) are of form $\beta^2 f(\theta, \phi, \mathbf{W}_{\text{RF}})$, where $f(\theta, \phi, \mathbf{W}_{\text{RF}})$ is a function not related to β . Thus, $\text{tr}(\mathbf{C}_{11})$ is of form $\beta^{-2} f(\theta, \phi, \mathbf{W}_{\text{RF}})$. As β is not a function of \mathbf{W} according to its definition, the solution of (12) is not a function of β . This completes the proof. ■

According to Lemma 1, β can be set to 1 in the following derivation without loss of generality. Further, if the range of the DOA to be estimated is known a priori, we can then optimize \mathbf{W}_{RF} to minimize the average CRB over that range. Denoting the prior ranges of the azimuth and elevation angles as $[\theta_b, \theta_u]$ and $[\phi_b, \phi_u]$, respectively, we uniformly sample them as follows

$$\begin{aligned} \theta_j &= \theta_b + \frac{(j-1)}{J}(\theta_u - \theta_b), \quad \text{for } j = 1, \dots, J, \\ \phi_k &= \phi_b + \frac{(k-1)}{K}(\phi_u - \phi_b), \quad \text{for } k = 1, \dots, K. \end{aligned} \quad (13)$$

Instead of solving the problem in (12), we optimize \mathbf{W}_{RF} aiming at minimizing the average CRB over the sampled DOA range subject to the unit modulus constraints. That is,

$$\begin{aligned} \underset{\mathbf{W}_{\text{RF}}}{\text{minimize}} \quad & f = \sum_{j=1}^J \sum_{k=1}^K \text{tr}(\mathbf{C}_{11}(\theta_j, \phi_k)) \\ \text{subject to} \quad & |[\mathbf{w}_{n,m}]_i| = 1, \quad \forall n, m, i. \end{aligned} \quad (14)$$

where $\mathbf{C}_{11}(\theta_j, \phi_k)$ corresponds to the one by replacing θ and ϕ with θ_j and ϕ_k in (11).

IV. MANIFOLD OPTIMIZATION ALGORITHM

It appears difficult to solve (14) because of not only the complicated objective function, but also the highly non-convex feasible set. Specifically, the analog beamformer $\mathbf{W}_{\text{RF},n}$ has a block diagonal structure and only the non-zero elements in the block matrices need to be optimized. Furthermore, they should satisfy the unit modulus constraint. To tackle these difficulties, we first introduce a sparse mask matrix $\mathbf{P} \in \mathbb{C}^{N_{\text{BS}} \times N_{\text{RF}} N}$ as

$$\mathbf{P}_{ij} = \begin{cases} 1 & [\mathbf{W}_{\text{RF}}]_{ij} \neq 0 \\ 0 & [\mathbf{W}_{\text{RF}}]_{ij} = 0, \end{cases} \quad (15)$$

then we can rewrite the analog beamformer in a form of $\mathbf{W}_{\text{RF}} = \mathbf{P} \odot \widetilde{\mathbf{W}}_{\text{RF}}$, where $\widetilde{\mathbf{W}}_{\text{RF}} \in \mathbb{C}^{N_{\text{BS}} \times N_{\text{RF}} N}$ is an auxiliary matrix variable without the block diagonal matrix constraint and all of its elements should satisfy the unit modulus constraints. Thus, the feasible set of $\widetilde{\mathbf{W}}_{\text{RF}}$ is essentially a typical Riemannian manifold [1], [12], i.e., $\mathcal{X} = \{\mathbf{X} \in \mathbb{C}^{N_{\text{BS}} \times N_{\text{RF}} N} : |[\mathbf{X}]_{ij}| = 1, \forall i, j\}$. Therefore, to minimize f with respect to $\widetilde{\mathbf{W}}_{\text{RF}}$ (instead of \mathbf{W}_{RF}) becomes a Riemannian optimization problem, which has been studied in [1], [12].

In this letter, we propose to extend the gradient-descent (GD) algorithm to minimize the objective in (14) over the Riemannian manifold. The basic idea is that in the i -th iteration, we first update the optimization variable $\widetilde{\mathbf{W}}_{\text{RF}}^{(i)}$ along the opposite direction of the *Riemannian gradient* to achieve a local minimizer on its *tangent space*, where the tangent space is a linear space composed of all the vectors that tangentially pass through $\widetilde{\mathbf{W}}_{\text{RF}}^{(i)}$, and the Riemannian gradient is the projection of the conjugate Euclidean gradient $\nabla f(\widetilde{\mathbf{W}}_{\text{RF}}^{(i)})$ onto the tangent space. Subsequently, we retract the minimizer

on the tangent space back to the manifold to obtain $\widetilde{\mathbf{W}}_{\text{RF}}^{(i+1)}$ as the finish of the iteration.

However, the application of manifold optimization is not straightforward and the conjugate Euclidean gradient needs to be derived first. Based on the differential rule $d(\mathbf{X}^{-1}) = -\mathbf{X}^{-1}d(\mathbf{X})\mathbf{X}^{-1}$, we have from (11)

$$\begin{aligned} d(\text{tr}(\mathbf{C}_{11})) &= \text{tr}(\text{Td}(\mathbf{F}_{11})) - \text{tr}(\text{Td}(\mathbf{F}_{12})\mathbf{F}_{22}^{-1}\mathbf{F}_{21}) \\ &\quad + \text{tr}(\mathbf{T}\mathbf{F}_{12}\mathbf{F}_{22}^{-1}d(\mathbf{F}_{22})\mathbf{F}_{22}^{-1}\mathbf{F}_{21}) - \text{tr}(\mathbf{T}\mathbf{F}_{12}\mathbf{F}_{22}^{-1}d(\mathbf{F}_{21})), \end{aligned} \quad (16)$$

where $\mathbf{T} = -(\mathbf{F}_{11} - \mathbf{F}_{12}\mathbf{F}_{22}^{-1}\mathbf{F}_{21})^{-2}$. We can further obtain from (10) that ¹

$$d(\mathbf{F}_{mn}) = \gamma \left(\mathbf{A}_m^H \mathbf{W}_{\text{RF}} d(\mathbf{W}_{\text{RF}}^H) \mathbf{A}_n + \mathbf{A}_m^T d(\mathbf{W}_{\text{RF}}^*) \mathbf{W}_{\text{RF}}^T \mathbf{A}_n^* \right),$$

where $\gamma \triangleq \frac{N_{\text{RF}}}{\sigma^2 N_{\text{BS}}}$. Substituting them into (16) and using the fact that $d(\mathbf{W}_{\text{RF}}) = \mathbf{P} \odot d(\widetilde{\mathbf{W}}_{\text{RF}})$ and $\text{tr}(\mathbf{A}(\mathbf{B} \odot \mathbf{C})) = \text{tr}((\mathbf{A} \odot \mathbf{B}^T)\mathbf{C})$ for arbitrary matrices \mathbf{A} , \mathbf{B} and \mathbf{C} , we have

$$\begin{aligned} d(\text{tr}(\mathbf{C}_{11})) &= \gamma \text{tr} \left(\left((\mathbf{A}_1 \mathbf{T} \mathbf{A}_1^H + \mathbf{A}_2 \mathbf{F}_{22}^{-1} \mathbf{F}_{21} \mathbf{T} \mathbf{F}_{12} \mathbf{F}_{22}^{-1} \mathbf{A}_2^H - \right. \right. \\ &\quad \left. \left. 2\text{Re}\{\mathbf{A}_2 \mathbf{F}_{22}^{-1} \mathbf{F}_{21} \mathbf{T} \mathbf{A}_1^H\}) \mathbf{W}_{\text{RF}} \odot \mathbf{P} \right) d(\widetilde{\mathbf{W}}_{\text{RF}}^H) \right). \end{aligned} \quad (17)$$

According to that $d(f(\widetilde{\mathbf{W}}_{\text{RF}})) = \text{tr}(\nabla f(\widetilde{\mathbf{W}}_{\text{RF}})d(\widetilde{\mathbf{W}}_{\text{RF}}^H))$, we obtain the Euclidean gradient from (17)

$$\nabla f(\widetilde{\mathbf{W}}_{\text{RF}}) = \gamma \sum_{j=1}^J \sum_{k=1}^K ((\mathbf{J}_{jk} + \mathbf{K}_{jk} - 2\text{Re}\{\mathbf{Q}_{jk}\}) \mathbf{W}_{\text{RF}}) \odot \mathbf{P}, \quad (18)$$

where

$$\begin{aligned} \mathbf{J}_{jk} &= (\mathbf{A}_1 \mathbf{T} \mathbf{A}_1^H)|_{\theta=\theta_j, \phi=\phi_k}, \\ \mathbf{K}_{jk} &= (\mathbf{A}_2 \mathbf{F}_{22}^{-1} \mathbf{F}_{21} \mathbf{T} \mathbf{F}_{12} \mathbf{F}_{22}^{-1} \mathbf{A}_2^H)|_{\theta=\theta_j, \phi=\phi_k}, \\ \mathbf{Q}_{jk} &= (\mathbf{A}_2 \mathbf{F}_{22}^{-1} \mathbf{F}_{21} \mathbf{T} \mathbf{A}_1^H)|_{\theta=\theta_j, \phi=\phi_k}. \end{aligned} \quad (19)$$

The Riemannian gradient can be obtained by projecting the Euclidean gradient onto the tangent space of $\widetilde{\mathbf{W}}_{\text{RF}}$, i.e.,

$$\text{grad} f(\widetilde{\mathbf{W}}_{\text{RF}}) = \nabla f(\widetilde{\mathbf{W}}_{\text{RF}}) - \text{Re}\{\nabla f(\widetilde{\mathbf{W}}_{\text{RF}}) \odot \widetilde{\mathbf{W}}_{\text{RF}}^* \odot \widetilde{\mathbf{W}}_{\text{RF}}\}. \quad (20)$$

With the derived Riemannian gradient, $\widetilde{\mathbf{W}}_{\text{RF}}$ in the i -th iteration is updated as follows

$$[\widetilde{\mathbf{W}}_{\text{RF}}^{(i)}]_{pq} = \frac{[\widetilde{\mathbf{W}}_{\text{RF}}^{(i-1)} + \alpha^{(i)} \mathbf{D}^{(i)}]_{pq}}{|[\widetilde{\mathbf{W}}_{\text{RF}}^{(i-1)} + \alpha^{(i)} \mathbf{D}^{(i)}]_{pq}|}, \quad (21)$$

where $\mathbf{D}^{(i)} = -\text{grad} f(\widetilde{\mathbf{W}}_{\text{RF}}^{(i-1)})$ and $\alpha^{(i)}$ denote the negative direction of Riemannian gradient and the Armijo backtracking step size, respectively. According to [14], [15], $\widetilde{\mathbf{W}}_{\text{RF}}$ is guaranteed to converge to a local minimum of $f(\widetilde{\mathbf{W}}_{\text{RF}})$ and satisfy the unit modulus constraints. The overall algorithm is summarized in Algorithm 1 and termed as CRB-MO, where ϵ is the convergence threshold. It is worth noting that as \mathbf{W} can be optimized offline, it thus does not lead to any extra computational complexity in the real-time implementation.

¹According to the differential rule [13], the term \mathbf{W}_{RF} is regarded as a constant matrix during the derivation of the conjugate gradient.

Algorithm 1 CRB-MO Algorithm

- 1: Randomly initialize $\widetilde{\mathbf{W}}_{\text{RF}}^{(0)}$ and set $i = 0$;
 - 2: **repeat**
 - 3: Compute the Riemannian gradient $\text{grad}f(\widetilde{\mathbf{W}}_{\text{RF}}^{(i)})$ according to (18) and (20);
 - 4: Update $\widetilde{\mathbf{W}}_{\text{RF}}^{(i+1)}$ according to (21);
 - 5: $i \leftarrow i + 1$;
 - 6: **until** $f(\widetilde{\mathbf{W}}_{\text{RF}}^{(i-1)}) - f(\widetilde{\mathbf{W}}_{\text{RF}}^{(i)}) \leq \epsilon$;
 - 7: $\mathbf{W}_{\text{RF}} = \mathbf{P} \odot \widetilde{\mathbf{W}}_{\text{RF}}^{(i)}$;
-

V. SIMULATION RESULTS

Throughout the simulations, we set $N_{\text{BS}} = 512$ ($P = 16$, $Q = 32$), $N_{\text{UE}} = 4$, $N_{\text{RF}} = 4$ and $N = 4$. Without loss of generality, a typical maximum likelihood (ML) based algorithm in [16] is adopted for DOA estimation with different receive beamformers, i.e., the traditional random beamformers and the beamformers optimized via proposed CRB-MO algorithm with $J = K = 180$ to guarantee sufficient angular resolutions. The mean square error (MSE) of the azimuth angle θ is adopted as the performance metric in the following figures, while the MSE of the elevation angle ϕ has been observed with similar result. The SNR is defined as $\frac{P}{\sigma^2}$. All the results were obtained from the average over 1000 independent channel realizations.

Fig. 1 shows the average MSE as a function of SNR in a typical mmWave communication scenario with $\theta \in [-\frac{\pi}{3}, \frac{\pi}{3}]$, $\phi \in [\frac{5\pi}{12}, \frac{7\pi}{12}]$ and $\alpha \sim \mathcal{CN}(0, 1)$. It is assumed that such DOA range is known a priori in the CRB-MO algorithm. We can see that with the optimized receive beamformers from the CRB-MO algorithm, the CRB is significantly improved by around 5dB in the required SNR over that with randomly generated beamformers. Meanwhile, the ML DOA algorithm with the optimized beamformers achieves similar performance improvement and approaches the CRB.

To better explain the phenomenon in Fig. 1, Fig. 2 further depicts the array power response, which is defined as $g(\phi) = |\mathbf{W}_{\text{BS}}(\theta, \phi)|$ with a fixed $\theta = \frac{\pi}{2}$, of the resulting beamformers of the two algorithms. We can see that the random beamformer exhibits a relatively flat power distribution in the whole angle domain. However, the proposed CRB-MO algorithm utilizes the prior information and generates a beam whose power is more concentrated on the specific DOA range. This provides some insight for the HBF design in the beam training stage for practical applications.

Fig. 3 further demonstrates the comparison result with $\theta \in [-\frac{\pi}{6}, \frac{\pi}{6}]$ and $\phi \in [\frac{5\pi}{12}, \frac{7\pi}{12}]$, which can be regarded as a scenario in the warm boot stage where one may have more accurate information about the DOA range. Compared to the result in Fig. 1, both algorithms achieve a lower MSE as the DOA range is narrowed. However, the CRB-MO algorithm achieves a higher gain due to the more specific prior information. This is because, as similar to that in Fig. 2, we observed a more concentrated power distribution with a narrower DOA range.

Finally, Fig. 4 depicts the estimation result in a typical two-path scenario, where the power of the NLoS path is -5dB lower than that of the LoS path [10]. The DOA ranges of the

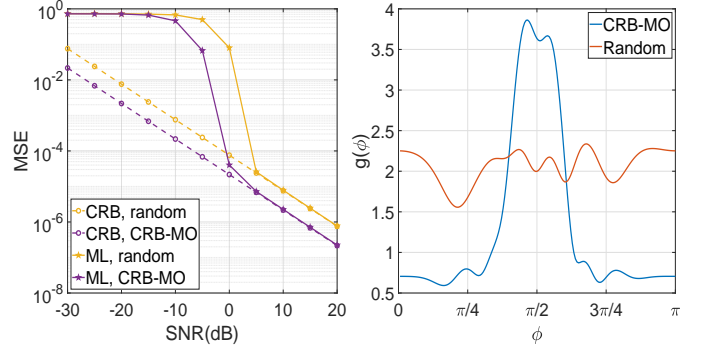


Fig. 1. MSE v.s. SNR for different HBF algorithms when $\theta \in [-\frac{\pi}{3}, \frac{\pi}{3}]$ and $\phi \in [\frac{5\pi}{12}, \frac{7\pi}{12}]$.

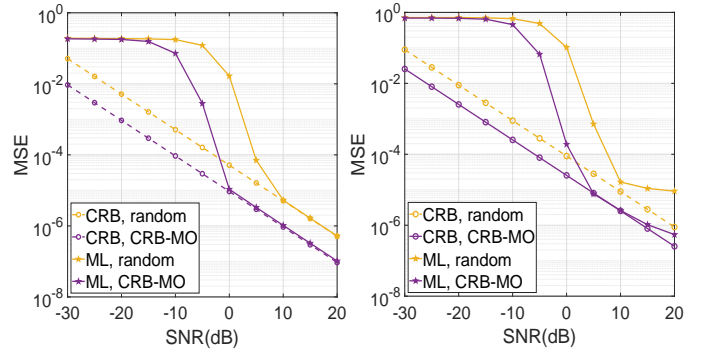


Fig. 2. Array power response $g(\phi)$ for different HBF algorithms.

two paths are set as follows: $\theta_0 \in [-\frac{\pi}{3}, \frac{\pi}{3}]$, $\phi_0 \in [\frac{5\pi}{12}, \frac{7\pi}{12}]$, $\theta_1 \in [-\frac{\pi}{2}, \frac{\pi}{2}]$ and $\phi_1 \in [0, \pi]$. For the CRB-MO algorithm, we only utilize the prior information of the LoS path. The CRB curves correspond to the joint estimation of the two paths based on the received signal, while the ML curves correspond to the DOA estimation of only the LoS path by taking the NLoS interference as part of the noise. Thus, at high SNRs, the ML curves become flat. However, it can be seen that the CRB-MO algorithm still significantly outperforms the random algorithm in the multi-path scenario. Although in this letter we focus on the DOA estimation of the LoS path, the proposed CRB-MO algorithm can also be extended to the beamformer design for the joint DOA estimation of the multiple paths.

VI. CONCLUSION

This letter proposed an HBF design approach for improving the DOA estimation performance based on the CRB analysis. By exploring the a priori information of the DOA range, we formulated an HBF optimization problem aiming at minimizing the average CRB over the prior DOA range subject to the constraint on the PC analog beamformer, and solved it by applying MO with guaranteed convergence. Simulation results have demonstrated the substantial performance improvement of the proposed CRB-MO algorithm over the conventional random beamforming.

REFERENCES

- [1] X. Yu, J. Shen, J. Zhang, and K. B. Letaief, "Alternating minimization algorithms for hybrid precoding in millimeter wave MIMO systems," *IEEE J. Sel. Topics Signal Process.*, vol. 10, no. 3, pp. 485–500, Apr. 2016.
- [2] O. E. Ayach, S. Rajagopal, S. Abu-Surra, Z. Pi, and R. W. Heath, "Spatially sparse precoding in millimeter wave MIMO systems," *IEEE Trans. Wireless Commun.*, vol. 13, no. 3, pp. 1499–1513, Mar. 2014.
- [3] D. Fan, F. Gao, Y. Liu, Y. Deng, G. Wang, Z. Zhong, and A. Nallanathan, "Angle domain channel estimation in hybrid millimeter wave massive MIMO systems," *IEEE Trans. Wireless Commun.*, vol. 17, no. 12, pp. 8165–8179, Oct. 2018.
- [4] F. Shu, Y. Qin, T. Liu, L. Gui, Y. Zhang, J. Li, and Z. Han, "Low-complexity and high-resolution DOA estimation for hybrid analog and digital massive MIMO receive array," *IEEE Trans. Commun.*, vol. 66, no. 6, pp. 2487–2501, Feb. 2018.
- [5] Z. Zheng, W. Wang, H. Meng, H. C. So, and H. Zhang, "Efficient beamspace-based algorithm for two-dimensional DOA estimation of incoherently distributed sources in massive mimo systems," *IEEE Trans. Veh. Technol.*, vol. 67, no. 12, pp. 11 776–11 789, Oct. 2018.
- [6] Z. Liu, Z. Huang, and Y. Zhou, "An efficient maximum likelihood method for direction-of-arrival estimation via sparse bayesian learning," *IEEE Trans. Wireless Commun.*, vol. 11, no. 10, pp. 1–11, Sept. 2012.
- [7] D. Fan, Y. Deng, F. Gao, Y. Liu, G. Wang, Z. Zhong, and A. Nallanathan, "Training based DOA estimation in hybrid mmwave massive MIMO systems," in *Proc. IEEE Global Commun. Conf. (GLOBECOM)*, 2017.
- [8] J. Lee, G. Gil, and Y. H. Lee, "Channel estimation via orthogonal matching pursuit for hybrid MIMO systems in millimeter wave communications," *IEEE Trans. Commun.*, vol. 64, no. 6, pp. 2370–2386, May 2016.
- [9] A. Alkhateeb, O. El Ayach, G. Leus, and R. W. Heath, "Channel estimation and hybrid precoding for millimeter wave cellular systems," *IEEE J. Sel. Topics Signal Process.*, vol. 8, no. 5, pp. 831–846, 2014.
- [10] X. Gao, L. Dai, S. Han, C. I, and X. Wang, "Reliable beamspace channel estimation for millimeter-wave massive MIMO systems with lens antenna array," *IEEE Trans. Wireless Commun.*, vol. 16, no. 9, pp. 6010–6021, Sept. 2017.
- [11] R. Zamir, "A proof of the Fisher information inequality via a data processing argument," *IEEE Trans. Inf. Theory*, vol. 44, no. 3, pp. 1246–1250, 1998.
- [12] T. Lin, J. Cong, Y. Zhu, J. Zhang, and K. Ben Letaief, "Hybrid beamforming for millimeter wave systems using the MMSE criterion," *IEEE Trans. Commun.*, vol. 67, no. 5, pp. 3693–3708, May 2019.
- [13] A. Hjørungnes, *Complex-Valued Matrix Derivatives*, Cambridge, U.K.: Cambridge Univ. Press, 2011.
- [14] N. Boumal, "An introduction to optimization on smooth manifolds," Nov 2020. [Online]. Available: <http://www.nicolasboumal.net/book>
- [15] P.-A. Absil, R. Mahony, and R. Sepulchre, *Optimization algorithms on matrix manifolds*. Princeton University Press, 2009.
- [16] J. Li and R. T. Compton, "Maximum likelihood angle estimation for signals with known waveforms," *IEEE Trans. Signal Process.*, vol. 41, no. 9, pp. 2850–2862, 1993.